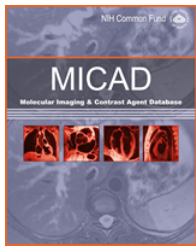




NLM Citation: Chopra A. Microbubbles with a disteroylphosphatidylcholine, disteroylphosphatidylethanolamine-polyethyleneglycol (PEG) 2000-pyridyldithio propionate-PEG 40 stearate shell conjugated to cyclic arginine-glycine-aspartic acid-d-tyrosine-lysine (cRGD) pentapeptide. 2011 Mar 28 [Updated 2011 Apr 28]. In: Molecular Imaging and Contrast Agent Database (MICAD) [Internet]. Bethesda (MD): National Center for Biotechnology Information (US); 2004-2013.

Bookshelf URL: <https://www.ncbi.nlm.nih.gov/books/>



Microbubbles with a disteroylphosphatidylcholine, disteroylphosphatidylethanolamine-polyethyleneglycol (PEG) 2000-pyridyldithio propionate-PEG 40 stearate shell conjugated to cyclic arginine-glycine-aspartic acid-d-tyrosine-lysine (cRGD) pentapeptide

cRGD-MB

Arvind Chopra, PhD¹

Created: March 28, 2011; Updated: April 28, 2011.

Chemical name:	Microbubbles with a disteroylphosphatidylcholine, disteroylphosphatidylethanolamine-polyethylene glycol (PEG) 2000-pyridyldithio propionate-PEG 40 stearate shell conjugated to cyclic arginine-glycine-aspartic acid-d-tyrosine-lysine (cRGD) pentapeptide	
Abbreviated name:	cRGD-MB	
Synonym:		
Agent Category:	Peptide	
Target:	$\alpha_v\beta_3$ integrin receptor	
Target Category:	Receptors	
Method of detection:	Ultrasound imaging	
Source of signal / contrast:	Microbubbles	
Activation:	No	
Studies:	<ul style="list-style-type: none">• <i>In vitro</i>• Rodents	
	Structure not available in PubChem.	

Background

[PubMed]

Ultrasonography (ultrasound) is a technique for the noninvasive imaging of tumors because it is easy to use, is relatively inexpensive compared to other imaging modalities, does not use radionuclides or x-rays, and produces

Author Affiliation: 1 National Center for Biotechnology Information, NLM, NIH, Bethesda, MD 20894; Email: micad@ncbi.nlm.nih.gov.

real-time images (1, 2). Imaging with this modality may involve the use of ultrasound contrast agents (UCA) based on microbubbles (MB), which are made up of a thin, biodegradable, lipid or polymeric shell filled with various types of gases, such as perfluorocarbon, sulphur hexafluoride, decafluorobutane, etc (3, 4). Because of their size and structural features, the MB cannot permeate the extracellular spaces, so they stay in the vascular circulation until the core gas diffuses into the blood and the remaining shell is metabolized (2). When exposed to a narrow range of ultrasound frequencies (3–5 MHz), the gas in the MB resonates with the sound; this in turn causes the MB to oscillate, which generates a signature acoustic echo (signal) that can be captured with a transducer and converted into a signal to generate an image. The application of ultrasound in medicine has been discussed in detail elsewhere (5).

Investigators have recently become interested in the use of targeted UCA for the detection of malignant tumors because these agents can be directed to bind to specific molecules that are overexpressed on the surface of cells in cancerous tissues (4). An additional advantage of using targeted UCA with ultrasonography is that malignant lesions can be visualized noninvasively, whereas tumors can be overlooked during a visual *ex vivo* examination of tissues obtained after a biopsy. Tumors with a malignant phenotype are known to show elevated angiogenic activity (development of new vasculature from old blood vessels), and endothelial cells in the vasculature of these lesions show increased expression of certain cell surface molecules such as $\alpha_v\beta_3$ integrins (6). The $\alpha_v\beta_3$ integrins are heterodimeric transmembrane cell adhesion molecules that are recognized biomarkers of angiogenesis, tumor progression, and metastasis, and they are overexpressed in a variety of cancers (6). Integrins are targeted by a variety of antagonist drugs that can prevent tumor progression (6), and they are also used with imaging agents, including UCA, for the noninvasive visualization of tumors (4).

Most targeted MB have traditionally been prepared with either avidin or biotin as the coupling agents, and these MB could not be used in the clinical setting because of their potential immunogenicity (4). In an effort to alleviate this problem, lipid-based (liposomal) MB with pyridylidithio propionate (PDP) on the surface were prepared and conjugated to a cyclic arginine-glycine-aspartic acid motif (cRGD) containing pentapeptide (such peptides are known to have a high affinity for $\alpha_v\beta_3$ integrins (7)) to generate cRGD-MB. The cRGD-MB were evaluated for use in imaging the cancerous lesion vasculature in mice bearing tumors generated with [bEnd.3 cells](#) (mouse endothelial cells that express $\alpha_v\beta_3$ integrins as confirmed with flow cytometry) (4).

Other Sources of Information

[MICAD](#) chapters related to integrins

Homo sapiens integrin alpha V, transcript variant 1, [protein](#) and [mRNA](#) sequences

Integrin alpha V in [Gene database](#), Gene ID: 3685

Homo sapiens integrin beta 3, [protein](#) and [mRNA](#) sequences

Integrin beta 3 in [Gene database](#), Gene ID: 374209

[Clinical trials](#) involving integrins

Integrins in [Online Mendelian Inheritance in Man \(OMIM\)](#) database

Integrin signaling pathways in [Pathway Interaction Database](#)

Synthesis

[PubMed]

MB with a disteroylphosphatidylcholine, disteroylphosphatidylethanolamine-polyethylene glycol (PEG) 2000-PDP-PEG 40 stearate shell (PDP-MB) were prepared as described by Anderson et al. (4). In some preparations,

~2% moles of Dil, a commercially available fluorescent membrane probe, was included in the reaction mixture for the detection of MB during *ex vivo* fluorescence microscopy. The PDP-MB were conjugated with the cRGD pentapeptide as detailed elsewhere (4). For some studies, MB containing a fluorescein isothiocyanate (FITC) derivative of cRGD (FITC-cRGD-MB) were prepared as described above. Control MB containing a non-binding scrambled cRAD pentapeptide (arginine-alanine-aspartic acid) were also prepared as described above.

The mean diameters of the control MB and the targeted MB were $2.75 \pm 0.02 \mu\text{m}$ and $2.71 \pm 0.01 \mu\text{m}$, respectively, and <2% of the MB had a diameter $>8.0 \mu\text{m}$. The concentrations of the control MB and the targeted MB in the final preparations were reported to be $133 \pm 8.0 \times 10^7/\text{mL}$ and $148 \pm 1.1 \times 10^7/\text{mL}$, respectively. Fluorescence spectroscopy of the FITC-cRGD-MB preparation revealed that $8.2 \pm 1.6 \times 10^6$ cRGD peptides were conjugated to each targeted MB.

In Vitro Studies: Testing in Cells and Tissues

[PubMed]

Parallel plate flow chamber assays showed that the adhesion of cRGD-MB to recombinant $\alpha_v\beta_3$ integrin substrates was significantly higher (37.5 ± 9.2 MB/field of view (FOV); $P < 0.01$) than adhesion to a casein surface (0.7 ± 0.5 MB/FOV) or to an $\alpha_v\beta_3$ integrin surface blocked with an anti- $\alpha_v\beta_3$ integrin antibody (3.9 ± 1.5 MB/FOV) (4). The cRAD-MB exhibited minimal binding to any one of these surfaces.

In another study in which bEnd.3 cells were exposed to cRGD-MB alone, the MB showed >5-fold higher binding than cRAD-MB, PDP-MB, and cells treated with antibodies blocking either the α_v or the β_3 integrin subunit (4). This indicated that the cRGD-MB bound specifically to the $\alpha_v\beta_3$ integrin receptors.

Animal Studies

Rodents

[PubMed]

Ultrasound imaging was performed on Friend leukemia virus B-sensitive inbred mice bearing metastatic breast cancer Met-1 cell tumors as described by Anderson et al. (4). The animals were administered cRGD-MB and either cRAD-MB ($n = 6$ mice) or PDP-MB ($n = 4$ mice) *via* bolus through the tail vein, and images were acquired in a random order from the animals in each group. There was a 5-min delay between each imaging session, and a high-power ultrasound pulse was introduced to destroy MB from the previous study. Ultrasound imaging was performed with a protocol that could distinguish between the contrast echoes obtained from the target-bound and the free circulating MB as detailed elsewhere (4). Application of a high-powered ultrasound destruction sequence at 7 min after injection was shown to minimize the signal obtained from any circulating MB; this time point was selected for comparison of images obtained from the different MB treatment groups. Images obtained from mice treated with cRGD-MB clearly showed the tumor size and border and were easily distinguished from baseline images obtained before treatment with the UCA. The accumulation of targeted MB in the tumor vasculature of these animals was confirmed *ex vivo* with confocal microscopy using Dil-cRGD-MB as described by Anderson et al. (4).

In another study, the binding specificity of cRGD-MB was investigated in mice bearing Met-1 cell tumors after the animals ($n = 6$) were treated with a monoclonal antibody (mAb) that blocked the $\alpha_v\beta_3$ integrins (4). The mice were administered cRGD-MB to establish baseline adhesion of the UCA in the tumors, and the animals were injected with ~700 pmol anti- $\alpha_v\beta_3$ integrin mAb at 5 min after injection of cRGD-MB. At 30 min after the mAb treatment, the animals were again injected with cRGD-MB, and ultrasound imaging was performed to assess binding of the MB to the target. The tumor image intensity obtained from the mAb-treated animals was

reported to be reduced by 3.2-fold compared to the intensity observed before the mAb treatment (baseline image). This indicated that the cRGD-MB bound specifically to the $\alpha_v\beta_3$ integrins.

Administration of the soluble cRGD pentapeptide (~1 μ mol) to the mice ($n = 10$) 30 min prior to the cRGD-MB injection did not block binding of the UCA to the tumor vasculature (4). The investigators have proposed several reasons for this observation, including rapid clearance of the peptide from the intravascular spaces due to its low molecular weight (~500 kDa), which may have reduced the local concentration of cRGD such that it was insufficient to block the $\alpha_v\beta_3$ integrin receptors (4).

On the basis of these results, the investigators concluded that the cRGD-MB had good binding specificity for the $\alpha_v\beta_3$ integrins and was a suitable UCA to visualize tumor angiogenesis (4).

Other Non-Primate Mammals

[\[PubMed\]](#)

No publications are currently available.

Non-Human Primates

[\[PubMed\]](#)

No publications are currently available.

Human Studies

[\[PubMed\]](#)

No publications are currently available.

Supplemental Information

[\[Disclaimers\]](#)

No information is currently available.

NIH Support

Supported by National Institutes of Health grants IR43CA137913, 2R44EB007857, R01CA134659, R01CA112356, and R01CA103828.

References

1. Eisenbrey J.R., Forsberg F. *Contrast-enhanced ultrasound for molecular imaging of angiogenesis*. . Eur J Nucl Med Mol Imaging. 2010;37 Suppl 1:S138–46. PubMed PMID: 20461376.
2. Wilson S.R., Burns P.N. *Microbubble-enhanced US in body imaging: what role?* . Radiology. 2010;257(1):24–39. PubMed PMID: 20851938.
3. Deshpande N., Needles A., Willmann J.K. *Molecular ultrasound imaging: current status and future directions*. . Clin Radiol. 2010;65(7):567–81. PubMed PMID: 20541656.
4. Anderson C.R., Hu X., Zhang H., Tlaxca J., Decleves A.E., Houghtaling R., Sharma K., Lawrence M., Ferrara K.W., Rychak J.J. *Ultrasound molecular imaging of tumor angiogenesis with an integrin targeted microbubble contrast agent*. . Invest Radiol. 2011;46(4):215–24. PubMed PMID: 21343825.
5. Moore C.L., Copel J.A. *Point-of-care ultrasonography*. . N Engl J Med. 2011;364(8):749–57. PubMed PMID: 21345104.

6. Desgrosellier J.S., Cheresh D.A. *Integrins in cancer: biological implications and therapeutic opportunities.* . Nat Rev Cancer. 2010;10(1):9–22. PubMed PMID: 20029421.
7. Liu S. *Radiolabeled cyclic RGD peptides as integrin alpha(v)beta(3)-targeted radiotracers: maximizing binding affinity via bivalence.* . Bioconjug Chem. 2009;20(12):2199–213. PubMed PMID: 19719118.